UCRL-17430

University of California

Ernest O. Lawrence Radiation Laboratory

RF RESONANCE OF IONIC-GROUND-STATE ATOMS OBSERVED THROUGH COLLISION-INDUCED COUPLING WITH METASTABLE-STATE NEUTRAL ATOMS

TWO-WEEK LOAN COPY

This is a Library Circulating Copy which may be borrowed for two weeks. For a personal retention copy, call Tech. Info. Division, Ext. 5545

Berkeley, California

DISCLAIMER

This document was prepared as an account of work sponsored by the United States Government. While this document is believed to contain correct information, neither the United States Government nor any agency thereof, nor the Regents of the University of California, nor any of their employees, makes any warranty, express or implied, or assumes any legal responsibility for the accuracy, completeness, or usefulness of any information, apparatus, product, or process disclosed, or represents that its use would not infringe privately owned rights. Reference herein to any specific commercial product, process, or service by its trade name, trademark, manufacturer, or otherwise, does not necessarily constitute or imply its endorsement, recommendation, or favoring by the United States Government or any agency thereof, or the Regents of the University of California. The views and opinions of authors expressed herein do not necessarily state or reflect those of the United States Government or any agency thereof or the Regents of the University of California.

Submitted to The Physical Review

UCRL-17430
Preprint

UNIVERSITY OF CALIFORNIA
Lawrence Radiation Laboratory
Berkeley, California

AEC Contract No. W-7405-eng-48

RF RESONANCE OF IONIC-GROUND-STATE ATOMS OBSERVED THROUGH COLLISION-INDUCED COUPLING WITH METASTABLE-STATE NEUTRAL ATOMS

Tetsuo Hadeishi and Chung-Heng Liu

March 14, 1967

RF RESONANCE OF IONIC-GROUND-STATE ATOMS OBSERVED THROUGH COLLISION-INDUCED COUPLING WITH METASTABLE-STATE NEUTRAL ATOMS

Tetsuo Hadeishi and Chung-Heng Liu

Lawrence Radiation Laboratory
University of California
Berkeley, California

March 14, 1967

ABSTRACT

The radiofrequency paragmagnetic-resonance method was used to observe the exchange collisions between the Xe ionic ground state $^2P_{3/2}$ and the neutral metastable state $^3P_2$. The ionic ground-state and metastable-state atoms are both formed and aligned by unidirectional low-energy high-flux electron-beam impact. The magnetic resonance of the ionic ground-state atoms was observed by monitoring changes in the transparency of the resonance radiation absorbed by the metastable-state atoms.

The experiment is described in detail, along with a possible process for observing this resonance. Phenomenological theories are presented which may explain the sign of the magnetic resonance signal of the ionic ground state compared with the metastable magnetic resonance.

I. INTRODUCTION

Atoms excited by unidirectional electron beams are, in general, aligned.[1] For excited states that decay by spontaneous emission of light, resonance radiations are therefore partially polarized. Magnetic resonances of excited states that cause alignment reduction change the polarization ratio of the emitted light. By this method, various properties of the excited states such as fine-structure separations, hyperfine-structure separations, g_J, g_F, and lifetimes have been measured.[2]

For metastable states formed and aligned by electron-impact excitation, atomic properties similar to those of the radiative excited states can be measured by monitoring the change in transparency of the resonance radiations absorbed by the metastable-state atoms.[3] Recently we reported that the ionic ground state of $Xe^+(^2P_{3/2})$ atoms, which is difficult to observe, can be studied optically by this metastable-state resonance-absorption method through collision-induced coupling with metastable-state atoms.[4] In this paper, we present more detailed information on experimental apparatus and improved theories that may describe the processes more accurately.

A high-flux, low-energy, unidirectional electron beam was produced by a space-charge-neutralization technique[4] using low-pressure Xe gas as a source of ions to neutralize the electron space charge. By this method, aligned ionic ground-state atoms of relatively high density, as well as metastable-state atoms, are formed. In a steady-state condition, a certain population equilibrium results for $Xe^+(^2P_{3/2})$ and $Xe(^3P_2)$ magnetic sublevels due to alignment by electron impact and

through subsequent spin-orbit coupling ionic ground-state--metastable-state collisions, collisions with the ground state of odd Xe isotopes, and the spin-lattice relaxation due to collision with walls, foreign gas atoms, and plasma discharge products. However, we may consider only the contribution to steady-state conditions that is due to the ionic ground-state--metastable-state collisions, since we can set our equipment to be sensitive to only this process, while all other processes appear as shortening of the spin-lattice relaxation time.

The magnetic resonance of the ionic ground state, at a sufficient rf power to equalize the population distribution, causes equilibrium population redistribution of the metastable state through subsequent exchange collisions to differ from cases in which no rf resonance field for Xe^+ is applied. Thus the changes in transparency of the resonance radiations absorbed by the metastable state allow us to observe rf resonance of the ionic ground state. The ionic-ground-state resonance signal is compared with the magnetic resonance signal of the metastable state.

II. ALIGNMENT OF EXCITED STATES

An elementary consideration of the process of electron-impact excitation demonstrates the principle behind the selective excitation of magnetic sublevels. In the Xe atom, the ground state has a $^1S_0$ configuration. Therefore, the initial level of the atom has zero orbital angular momentum (we assume nuclear spin is zero). The anisotropic excitation of excited states is based on the cylindrical symmetry that exists about the electron-beam axis.

Let us assume that in an inelastic collision the total spin and total angular momentum are separately conserved. Assume the angular momentum of the incident electron to be zero. Then the angular momentum of the electron, after exciting M_L of the excited level, must be equal to $-\hbar M$. If the incident electron possesses just enough energy to excite the atom from the $^1S_0$ ground state to the excited state, then $-\hbar M$ must equal zero since the velocity of the electron after collision is zero. Therefore, the excited state of the atom is expected to be in the $M_L = 0$. At the higher energy, using the Born approximation and neglecting electron spin, we can write

$$\sigma_{mn}(\theta)\, d\omega \propto \left| \iint V(\underset{\sim}{r}, \underset{\sim}{R}) \exp\{i(k_{mn}\underset{\sim}{n}_1 - k\underset{\sim}{n}_0) \cdot \underset{\sim}{R}\}\, \psi_n(\underset{\sim}{r})\psi_m(\underset{\sim}{r})\, d\underset{\sim}{r}\, d\underset{\sim}{R} \right|^2 d\omega, \tag{1}$$

where $k\hbar\underset{\sim}{n}_0$ and $k_{mn}\hbar\underset{\sim}{n}_1$ are the linear momentum of the electron before and after the impact, ψ_m and ψ_n are the initial- and final-state wave functions and $V(\underset{\sim}{r}, \underset{\sim}{R})$ is the Coulomb-interaction energy.[5] By choosing $\underset{\sim}{K} = k_{mn}\underset{\sim}{n}_1 - k\underset{\sim}{n}_0$ as the axis of quantization, we see that the $M_L = 0$ state is the only state we can expect to be excited, corresponding physically to the inability of the incident electron, whose momentum loss is along $\underset{\sim}{K}$, to exert a torque on the atomic electron about his axis.[6] For high energies, $\underset{\sim}{K}_1$ is perpendicular to $k\underset{\sim}{n}_0$ since $|k_{mn}\underset{\sim}{n}_1| \cong |k\underset{\sim}{n}_0|$. Therefore, should the excited state be the nP state, the state produced is given b $\mathcal{D}(0, \pi/2, 0)\,|0\rangle = (2)^{-1/2}[\,|1\rangle + |-1\rangle\,]$, and hence $M_L = 1$ and -1 states are produced by high-energy electron impact.

To treat the problem more rigorously is extremely complex since we must consider electron exchange, spin-orbit, and hyperfine

interactions. Recently, Percival and Seaton have carried out more rigorous calculations, including the above-mentioned interaction.[8]

Since the success of our experiment is based only on the existence of the population differences between magnetic sublevels, no detailed knowledge of the process of the excitation is needed. However, it is necessary to obtain a high density of aligned ionic ground-state and metastable-state atoms so that the effect is observable. This requires high-flux, unidirectional electron beams, as well as low-energy, if we are also to approximately satisfy the threshold-energy condition.

III. THEORY

The relevant energy-level diagram is shown in Fig. 1. By electron-impact excitation, the magnetic sublevels of $Xe^+(^2P_{3/2})$ and $Xe(^3P_2)$ are selectively excited. By electron impact, the magnetic sublevels $m_J = \pm 1/2$ of $Xe^+(^2P_{3/2})$ and $m_J = \pm 1$ and 0 of $Xe(^3P_2)$ should be selectively excited at the energy of the corresponding threshold energy of excitation. However, since we expect no threshold-energy condition to be rigorously satisfied, we assign the production rates α, β, and γ for the magnetic sublevels $m_J = \pm 2$, ± 1, and 0 of $Xe(^3P_2)$. Similarly, we assign the production rate α' and β' for the magnetic sublevels $m_J = \pm 3/2$ and $\pm 1/2$ of $Xe^+(^2P_{3/2})$. Since the electron-impact excitation aligns only the excited atoms, the production rate for m_J is the same for $-m_J$.

The metastable-state and ionic ground-state spin-relaxation times T_R and T_r represent the process that tends to cause the magnetic sublevel population to reach its thermal-equilibrium distribution by

collisions with the container wall, electrodes, and impurities, etc. excluding the process involving interaction with metastable ionic ground-state collisions.

Couplings between the metastable-state atoms and the ionic ground-state atom magnetic sublevels are induced through collisions. Equilibrium between the two systems is established in the characteristic time $\tau_2 \approx 1/\sigma vN$ for the ionic ground state, and $\tau_1 \cong 1/\sigma vn$ for the metastable state, where σ, v, N, and n are respectively the total-exchange cross section (spin exchange and spin exchange associated with charge exchange), relative velocity, metastable-state atom density, and ionic ground-state atom density.

In addition to ionic ground-state--metastable-state collisions, we should consider the exchange collisions with $^1S_0$ isotopic atoms whose nuclear spins are not zero as well as collisions of atoms having the same configuration. For a simplicity, we include such processes in T_R and T_r. We further assume that, due to collisions between $Xe^+(^2P_{3/2})$ and $Xe(^3P_2)$, the angular momentum changes at most one unit per collision.

Let N_2, N_1, N_0, N_{-1}, and N_{-2} be the population densities of the magnetic sublevels of $Xe(^3P_2)$ corresponding to M_J = 2, 1, 0, -1, and -2. Similarly, let $n_{3/2}$, $n_{1/2}$, $n_{-1/2}$, and $n_{-3/2}$ be the population densities of the magnetic sublevels of $Xe^+(^2P_{3/2})$ corresponding to M_J = 3/2, 1/2, -1/2, and -3/2. From these assumptions, we construct the following rate equations:

$$\frac{dN_2}{dt} = -\Sigma' N_2 W_{2j} + \Sigma' N_j W_{j2} - \frac{1}{\tau} N_2 + \alpha - v\sigma [N_1 \frac{n}{2} - N_2(n-n_{3/2})], \quad (2)$$

$$\frac{dN_1}{dt} = -\Sigma' N_1 W_{1j} + \Sigma' N_j W_{j1} - \frac{1}{\tau} N_1 + \beta - v\sigma[-N_1 n + N_2(n - n_{3/2}) + N_0 \frac{n}{2}], \quad (3)$$

$$\frac{dN_0}{dt} = -\Sigma' N_0 W_{0j} + \Sigma' N_j W_{j0} - \frac{1}{\tau} N_0 + \gamma - v\sigma[N_1 \frac{n}{2} + N_{-1} \frac{n}{2} - N_0 n], \quad (4)$$

$$\frac{dN_{-1}}{dt} = -\Sigma' N_{-1} W_{-1j} + \Sigma' N_j W_{j-1} - \frac{1}{\tau} N_{-1} + \beta - v\sigma[-N_{-1} n + N_{-2}(n - n_{3/2}) + N_0 \frac{n}{2}], \quad (5)$$

$$\frac{dN_{-2}}{dt} = -\Sigma' N_{-2} W_{-2j} + \Sigma' N_j W_{j-2} - \frac{1}{\tau} N_{-2} + \alpha - v\sigma[N_{-1} \frac{n}{2} - N_{-2}(n - n_{3/2})], \quad (6)$$

$$N = \sum_{j=-2}^{+2} N_j \quad (7)$$

and

$$n = \sum_{j=-3/2}^{3/2} n_j \quad (8)$$

where Σ' denotes the summation with W_{jj} to be avoided, N the total metastable-state density, n the total ionic ground-state density, τ the relaxation rate to other configuration states (such as the $^1S_0$ ground state and the neighboring $^1P_1$ state that decays to the ground state by spontaneous emission of light), W_{ij} the spin-relaxation rates between magnetic sublevels i and j (similar to the spin-lattice relaxation rate commonly used in solid-state physics[7]), v the relative velocity between $Xe(^3P_2)$ and $Xe^+(^2P_{3/2})$, and σ the exchange-collision cross section. For simplicity we assume a uniform relaxation rate, and write $W = W_{ij}$,

where i and j run from -2 to +2, with $W_{jj} = 0$. Then, in a steady state, we have

$$-4N_2 + N_1 + N_0 + N_{-1} + N_{-2} = \frac{N_2}{W\tau} - \frac{\alpha}{W} - \frac{v\sigma}{W}[N_1 \frac{n}{2} - N_2(n-n_{3/2})] \tag{9}$$

$$N_2 - 4N_1 + N_0 + N_{-1} + N_{-2} = \frac{1}{W\tau} N_1 - \frac{\beta}{W} - \frac{v\sigma}{W}[-N_1 n + N_2(n-n_{3/2}) + N_0 \frac{n}{2}] \tag{10}$$

$$N_2 + N_1 - 4N_0 + N_{-1} + N_{-2} = \frac{1}{W\tau} N_0 - \frac{\gamma}{W} - \frac{v\sigma}{W}[N_1 \frac{n}{2} + N_{-1} \frac{n}{2} - N_0 n], \tag{11}$$

$$N_2 + N_1 + N_0 - 4N_{-1} + N_{-2} = \frac{1}{W\tau} N_{-1} - \frac{\beta}{W} - \frac{v\sigma}{W}[-N_{-1} n + N_{-2}(n-n_{3/2}) - N_0 \frac{n}{2}], \tag{12}$$

and

$$N_2 + N_1 + N_0 + N_{-1} - 4N_{-2} = \frac{1}{W\tau} N_{-2} - \frac{\alpha}{W} - \frac{v\sigma}{W}[N_{-1} \frac{n}{2} - N_{-2}(n-n_{3/2})]. \tag{13}$$

Adding Eqs. (9), (10), (11), (12), and (13) gives us

$$N_2 + N_1 + N_0 + N_{-1} + N_{-2} = \tau(2\alpha + 2\beta + \gamma) = N , \tag{14}$$

satisfying the conservation of particles. Subtracting each of the above five equations from Eq. (14) and noting that $N_1 = N_{-1}$ and $N_2 = N_{-2}$, we have

$$-5N_2 = N - \frac{1}{W\tau} N_2 + \frac{\alpha}{W} + \frac{v\sigma}{W}[\frac{n}{2} N_1 - (n-n_{3/2})N_2] \tag{15}$$

$$5N_1 = N - \frac{1}{W\tau} N_1 + \frac{\beta}{W} + \frac{v\sigma}{W}[-nN_1 + (n-n_{3/2})N_2 + \frac{n}{2} N_0], \tag{16}$$

and

$$5N_0 = N - \frac{1}{W\tau} N_0 + \frac{\gamma}{W} + \frac{v\sigma}{W}[nN_1 - nN_0]. \tag{17}$$

Solving Eqs. (15), (16), and (17) we get

$$N_2 = \frac{N + \frac{\alpha}{W}}{5 + \frac{1}{W\tau} + \frac{v\sigma}{W}(n-n_{3/2})} + \frac{1}{2}\,\frac{N\,\frac{v\sigma}{W}}{5 + \frac{1}{W\tau} + \frac{v\sigma}{W}(n-n_{3/2})}\,N_1, \quad (18)$$

$$N_1 = \frac{\left\{(N+\frac{\beta}{W}) + \frac{\frac{v\sigma}{W}(n-n_{3/2})(N+\frac{\alpha}{W})}{5+\frac{1}{W\tau}+\frac{v\sigma}{W}(n-n_{3/2})} + \frac{1}{2}\,\frac{\frac{nv\sigma}{W}(N+\frac{\gamma}{W})}{5+\frac{1}{W\tau}+\frac{nv\sigma}{W}}\right\}}{\left\{5+\frac{1}{W\tau}+\frac{nv\sigma}{W} - \frac{1}{2}\,\frac{n(n-n')\frac{v^2\sigma^2}{W^2}}{5+\frac{1}{W\tau}+\frac{v\sigma}{W}(n-n_{3/2})} - \frac{1}{2}\,\frac{n^2\,\frac{v^2\sigma^2}{W^2}}{5+\frac{1}{W\tau}+\frac{nv\sigma}{W}}\right\}}, \quad (19)$$

and

$$N_0 = \frac{N + \frac{\gamma}{W}}{5 + \frac{1}{W\tau} + \frac{nv\sigma}{W}} + \frac{\frac{nv\sigma}{W}}{5 + \frac{1}{W\tau} + \frac{nv\sigma}{W}}\,N_1 . \quad (20)$$

III. A. MAGNETIC RESONANCE OF $^3P_2$ METASTABLE STATE

We shall first calculate the magnetic resonance signal of $^3P_2$ metastable state. For the sake of simplicity, we shall neglect the contribution from exchange collisions.

Table I shows the relative absorption probabilities for linearly polarized light corresponding to $^3P_2$ - $^3S_1$ electric-dipole transitions. When the electron-beam axis is parallel to the externally applied magnetic field H_0 and the oscillating rf magnetic field perpendicular to it, the change of absorption of the incident resonance polarized linearly parallel to H_0 due to the magnetic resonance of the $^3P_2$ metastable state is

$$\text{signal}_{\parallel} \propto 8(\Delta N_0) + (2)(6)(\Delta N_1) \cong -\frac{4}{5}(\gamma + \beta - 2\alpha)\frac{1}{W} \quad (21)$$

where

$$\Delta N_1 \equiv (N_1)_{\text{rf resonance}} - (N_1)_{\text{steady state}} \cong \frac{N}{5} - \frac{N + \frac{\beta}{W}}{5 + \frac{1}{W\tau} + \frac{nv\sigma}{W}}$$

$$\cong \frac{1}{25W}(2\alpha + \gamma - 3\beta), \quad (22)$$

$$\Delta N_0 \equiv (N_0)_{\text{rf resonance}} - (N_0)_{\text{steady state}} \cong \frac{N}{5} - \frac{N + \frac{\gamma}{W}}{5 + \frac{1}{W\tau} + \frac{nv\sigma}{W}}$$

$$\cong \frac{1}{25W}(2\alpha + 2\beta - 4\gamma), \qquad (23)$$

if we neglect the term that arises from collisions. When the incident linearly polarized resonance radiation is polarized perpendicular to H_0, the change of the absorption is given by

$$\text{signal}_{\perp} \propto 1(\Delta N_0) + (2)(3)(\Delta N_1) + (2)(6)(\Delta N_2) = \frac{2}{25W}(7\gamma + 4\beta - 11\alpha), \qquad (24)$$

since

$$\Delta N_2 \equiv (N_2)_{\text{rf resonance}} - (N_2)_{\text{steady state}} \cong \frac{N}{5} - \frac{N + \frac{\alpha}{W}}{5 + \frac{1}{W\tau} + \frac{v\sigma}{W}(n - n_{3/2})}$$

$$\cong \frac{1}{25W}(2\beta + \gamma - 3\alpha). \qquad (25)$$

III. B. MAGNETIC RESONANCE OF $Xe^+(^2P_{3/2})$

Since the energy of the incident electron we used is only about 3 electron volts above the threshold energy of excitation for the $^3P_2$ state, we expect γ and $\beta > \alpha$. Therefore, we see from Eq. (21) and (24) that the absorption of the linearly polarized light parallel to the magnetic field decreases as the magnetic resonance condition for $^3P_2$ is satisfied and in the case of the linearly polarized light being perpendicular to the magnetic field, the resonance absorption increases.

For the magnetic resonance of $Xe^+(^2P_{3/2})$, we find $n_{3/2} = n/4$, if the oscillating rf magnetic field is sufficiently strong. Then, from Eqs. (18), (19), and (20) we get

$$\Delta N_2 \equiv (N_2)_{\text{at } n_{3/2} = \frac{n}{4}} - (N_2)_{\text{steady state}}$$

$$\cong \frac{N + \frac{\alpha}{W}}{(5 + \frac{1}{W\tau})^2}\left(\frac{1}{4}n - n_{3/2}\right)\frac{v\sigma}{W} + 0(v^2\sigma^2), \qquad (26)$$

$$\Delta N_1 \equiv (N_1)_{\text{at } n_{3/2} = \frac{n}{4}} - (N_1)_{\text{steady state}}$$

$$\simeq - \frac{N + \frac{\alpha}{W}}{(5 + \frac{1}{W\tau})^2} (\frac{1}{4} n - n_{3/2}) + 0(v^2\sigma^2), \tag{27}$$

and

$$\Delta N_0 \equiv (N_0)_{\text{at } n_{3/2} = \frac{n}{4}} - (N_0)_{\text{steady state}} \simeq 0 + 0(v^2\sigma^2) \simeq 0. \tag{28}$$

Therefore, the signal strengths of $Xe^+(^2P_{3/2})$ ionic ground-state resonances are given (to the first order of σv) by

$$\text{signal}_{\parallel} \propto 8(\Delta N_0) + (2)(6)(\Delta N_1)$$

$$= -12 \frac{N + \frac{\alpha}{W}}{(5 + \frac{1}{W\tau})^2} (\frac{1}{4} n - n_{3/2}) \frac{v\sigma}{W} \simeq - \frac{12}{25} (\frac{1}{4} n - n_{3/2}) \frac{Nv\sigma}{W} \tag{29}$$

$$\text{signal}_{\perp} \propto 1(\Delta N_0) + (2)(3)(\Delta N_1) + 2(6)\Delta N_2 \simeq + 6 \frac{N + \frac{\alpha}{W}}{(5 + \frac{1}{W\tau})^2} (\frac{1}{4} n - n_{3/2}) \frac{v\sigma}{W}$$

$$\simeq \frac{6}{25} (\frac{1}{4} n - n_{3/2}) \frac{Nv\sigma}{W} . \tag{30}$$

Thus, the sign of the signal depends on $n_{3/2} \gtrless n/4$.

It is interesting to compare the signal strength of $Xe^+(^2P_{3/2})$ and $Xe(^3P_2)$. Taking the ratio between Eq. (29) and Eq. (21), we can write

$$\frac{\text{signal}_{\parallel} [Xe^+(^2P_{3/2})]}{\text{signal}_{\parallel} [Xe(^3P_2)]} = \frac{\frac{3}{5}(\frac{1}{4} n - n_{3/2}) NV\sigma}{(\gamma + \beta + 2\alpha)} \tag{31}$$

$$\frac{\text{signal}_{\parallel} [Xe^+(^2P_{3/2})]}{\text{signal}_{\parallel} [Xe(^3P_2)]} \simeq \frac{1}{8} n\tau v\sigma \approx \frac{1}{10},$$

since we expect $\beta \simeq \gamma/2$, $\alpha \approx 0$, $n \approx 10^{11}$ atoms/cc, $\tau \simeq 10^{-3}$ sec, $V \simeq 10^5$ cm/sec, and $\sigma \approx 10^{-13}$ cm^2.

IV. EXPERIMENTAL CONSIDERATIONS

A. Production of a High-Flux Electron Beam

In order to obtain a detectable signal, the following conditions should be met.

(1) The electron beam should be unidirectional; therefore, gas pressure should be low to avoid multiple scattering of the electron beam.

(2) The electron-beam current density should be high.

The maximum electron current that can flow from a "hot" cathode to an anode in high vacuum is limited by the space charge of the electron, so that the current under such conditions is too small to produce a sufficient concentration of atoms in the metastable and ionic ground states. However, from Langmuir's theory[9] of space-charge-neutralized electron flow, we know that if even a small amount of gas is present and the applied voltage is higher than the ionization potential, the positive ions formed tend to neutralize the electron space charge, and thus allow the current to increase until it is limited only by the electron emission of the cathode, which depends upon the cathode temperature. Under conditions of space-charge neutralization, the cathode is surrounded by the ion sheath, and the rest of the volume is filled by a nearly field-free plasma. The voltage difference between the cathode and anode is concentrated between the cathode and ion sheath, so that the electrons receive most of their acceleration between the cathode and sheath, and enter the relatively field-free plasma perpendicular to the cathode surface.

Thus, by the space-charge neutralization method, the requirement of unidirectional high-electron current can be satisfied. Since the very ions that space-charge neutralize are formed by unidirectional electron

impact, we expect selective excitation of Zeeman magnetic sublevels just as the magnetic sublevels of the neutral metastable state atoms are selectively excited.

B. Apparatus

The experimental apparatus is almost identical to that used in our previous Ne metastable-state experiment,[3] with slight improvements in optical arrangement and the electronic detection system. Figure 2 is a block diagram of the experimental arrangement.

Resonance-absorption light is split into two beams, polarized parallel and perpendicular to each other, and is detected by RCA 7102 photomultiplier tubes. The difference of the output voltages from the two photomultiplier tubes is fed into the differential input of a PAR low-noise amplifier powered by mercury batteries. The difference of two photomultiplier output voltages is used mainly to reduce the effect due to light fluctuation of the lamp and thus avoid saturation of the preamplifier. To eliminate the inhomogeneous magnetic field generated by the indirect heater for the cathode of the electron gun, the heater current is turned on and off at 50 Hz, and the signal from the preamplifier is detected only when no heater current is flowing into the heater wire.

The radio frequency is amplitude-modulated at an audio frequency of about 550 Hz, and the amplitude-detection method is used with a phase-sensitive detector. However, the exchange-collision signals were too small to be observed by the phase-sensitive detector alone, so a digital integrator system was incorporated. This enabled us to sweep over the resonance curve several times, adding the successive resonance curves until the signal-to-noise ratio was sufficiently high.[7]

The electron tube is a simple diode structure consisting of a 3/4-in.-diam, indirectly heated Phillips cathode and an anode made of a 35-mil thick, 1-in.-diam Ta disc, spot-welded to a tungsten rod which extends through the Pyrex tube envelope. Cathode-anode separation is 2 cm. The electron tube was carefully processed by baking at 400° C for about 8 h before and after cathode activation under a vacuum pressure of about 3×10^{-9} mm of Hg. All electrodes were rf-bombarded at about 500° C for about 2 h. After activation, the heat-shielded cathode was operated at 1050° C with a heater input power of 50W. The bifila-wound indirect-heating element was constructed of a 20-mil tungsten wire coated with Alundum (Al_2O_3) by the cataphoresis process.

After tube activation, reagent-type Xe gas was introduced into the tube, which was then operated for a few hours. It was flushed several times, saturating the electrodes with Xe gas to minimize the ion-pumping effect. After several flushings, Xe gas at the desired pressure was introduced into the tube and the tube was sealed off. Ordinarily, the tube can be operated almost continuously for several months without any noticeable sign of deterioration. Using the Phillips cathode, we found it possible to expose the tube to the air for short

periods without any noticeable sign of a drop in emission. Although a complete reactivation cycle of the tube is necessary after each exposure to the air, the same sealed-off electron tube can be reopened to change the gas pressure.

An electrodeless discharge of Xe gas was used as a resonance-radiation light source. A quartz tube (8 mm i. d. and 10 cm long), filled with Xe at a pressure of about 0.9 mm of Hg, was placed in a coaxial resonance cavity driven by a diathermy microwave generator at about 2450 MHz. Maximum power output of the microwave generator used is about 100W. Although light intensity was high at maximum power output, it was necessary to operate at lower power in order to prevent melting of the quartz tubing by the heat generated by the discharge. Because of the relatively hard driving of the discharge, the lamp usually lasted only about 150 hours. Frequent replacements of the lamp were required although considerable care was taken in making the lamp by heating the quartz tubing to about 1000° C, as well as rf-discharging it while it was connected to the pump station during several Xe gas flushings. The reason for this may be that the temperature of the sealed-off lamp under the microwave discharge in the cavity was higher than the temperature it reached during its processing in the pump station, so that further ourgassing of the quartz tubing took place, while He gas diffused into the tube. Since the gas-filled tube is very simple to construct, we made no further improvement on the lamp.

The resonance radiation at 8409 Å, corresponding to the $^3S_1$-$^3P_2$ transition, was filtered by a narrow-band interference filter at about 35% transmission with a bandwidth of 15 Å. Two RCA 7102 photomultiplier tubes were used for light detection. No liquid-nitrogen cooling

was used, although we believe this would be desirable since the time-averaging system we used can overcome the tube-noise problem.

V. EXPERIMENTAL RESULTS

Figures 3 and 4 show the optical absorption of the cell or a function of the applied magnetic field, with about 8 hours of time-averaging. The magnetic-field value was calibrated from a metastable-state resonance of the even isotope of Xe whose g_J value is known from the atomic-beam magnetic resonance[10] to be 1.50089 ± 0.00006. The identification of $Xe^+(^2P_{3/2})$ magnetic resonance is made by noting its resonance positions corresponding to the calculated value of g_J with respect to the g_J and g_F values of the metastable state of even and odd isotopes of Xe. The signals shown in Fig. 3 are correlated with resonances in the $Xe(^3P_2)$ and $Xe^+(^2P_{3/2})$ state of even isotopes. These signals were observed by a single photomultiplier tube, instead of the two shown in Fig. 2, in order to check our prediction of the signals according to Eq. (21) and (24). It was found that the observed signals were in complete agreement with our prediction. Figure 4 shows the magnetic resonances, at a higher rf power level than that shown in Fig. 3, of odd isotopes of $Xe^{129}(^3P_2)$, $Xe^{131}(^3P_2)$ and even isotopes of $Xe^+(^2P_{3/2})$ showing a power dip, in addition to a resonance corresponding to $g = 1.2530 \pm 0.0040$ that is not yet identified. Measured values of $Xe^{129}(^3P_2)$ with $J = 2$, $I = 1/2$, $F = 5/2$ and $Xe^{131}(^3P_2)$ with $J = 2$, $I = 3/2$, and $F = 3/2$ are both 1.2007 ± 0.004. Figure 5 shows a magnetic resonance corresponding to $g_F = 1.7986 \pm 0.0023$, which belongs to Xe^{129} with $F = 3/2$.

It is interesting that the relative signs of its signal between $Xe(^3P_2)$ and $Xe^+(^2P_{3/2})$ are opposite each other. From Eqs. (21), (25), (29), and (30), we conclude that $n_{3/2}$ is greater than n/4. We believe some detailed theoretical calculation is necessary to find a possible reason for this.

VI. CONCLUSION

Using relatively simple apparatus, we have readily observed the ionic ground state, which is very difficult to observe by more conventional methods. Our method should work with a variety of easily vaporized atoms given the value J is greater than 1/2 for the ionic ground state. An additional advantage over the conventional spin-exchange method is that we need only one collision to observe rf resonance, while the older method demands at least two, thus requiring relatively long spin-relaxation times of colliding species or higher pressure.

At present we are performing an experiment to identify the state that corresponds to $g = 1.2532 \pm 0.0004$ by observing emission lines from the cell. We believe that the signal is due to cascading from the long-lived excited state that decays to the short lived intermediate state by emitting infrared light, and that it decays to the metastable state via the short-lived intermediate state while maintaining its initial alignment because of electron-impact excitation.

We are also constructing an apparatus that should enable us to observe directly the resonance absorption of ultraviolet light by $Xe^+(^2P_{3/2})$ to prove that the effect we have observed is due to $Xe^+(^2P_{3/2})$ beyond any doubt.

We would like to thank Professor Howard Shugart of our group for discussions of this experiment, Dr. William Cooper of Project Sherwood at LRL Berkeley for stimulating discussion on the behavior of plasmas, and Professor Kenneth Watson and his students for discussions of collision theory.

REFERENCES

*This work was supported by the U. S. Atomic Energy Commission.

1. H. W. B. Skinner and E. T. S. Appleyard, Proc. Roy. Soc. (London) A117, 224 (1928).
2. W. E. Lamb, Phys. Rev. 105, 554 (1957); W. E. Lamb and T. H. Mainen, Phys. Rev. 105, 573 (1957). J. C. Pebay-Peyroula J. Phys. Rad. 20, 669 (1959).
3. H. G. Dehmelt, Phys. Rev. 103, 1125 (1956); T. Hadeishi, O. McHarris, and W. A. Nierenberg, Phys. Rev. 138, A983 (1965).
4. T. Hadeishi and C. -H. Liu, Phys. Rev. Letters 17, 513 (1966).
5. M. F. Mott and H. S. W. Massey, The Theory of Atomic Collisions (Clarendon Press, Oxford, 1961), 2nd ed.
6. L. I. Schiff, Quantum Mechanics (McGraw-Hill Book Co. Inc., New York, 1955), 2nd ed., p. 208.
7. See, for example, E. R. Andrew, Nuclear Magnetic Resonance (University Press, Cambridge, 1956), p. 213.
8. I. C. Percival and M. J. Seaton, Phil. Trans. Roy. Soc. (London) 251, 113 (1958).
9. I. Langmuir, Phys. Rev. 33, 954 (1929).
10. H. Friedburg and H. Kuiper, Naturwiss. 44, 487 (1957).

Table I. Relative absorption probabilities between magnetic sublevels M_J of $^3P_2$ and M'_J of $^3S_1$ of Xe.

Polarized light parallel to electron-beam direction

M'_J \ M_J	2	1	0	-1	-2
1	0	$\frac{1}{10}$	0	0	0
0	0	0	$\frac{2}{15}$	0	0
-1	0	0	0	$\frac{1}{10}$	0

Polarized light perpendicular to electron-beam direction

M'_J \ M_J	2	1	0	-1	-2
1	$\frac{1}{10}$	0	$\frac{1}{60}$	0	0
0	0	$\frac{1}{20}$	0	$\frac{1}{20}$	0
-1	0	0	$\frac{1}{60}$	0	$\frac{1}{10}$

FIGURE LEGENDS

Fig. 1. Relevant energy level diagram

Fig. 2. Block diagram of the experimental apparatus

Fig. 3. Magnetic resonance of $Xe(^3P_2)$ and $Xe^+(^2P_{3/2})$ using a single photomultiplier tube with an rf frequency of 5.085 MH_z

Fig. 4. Magnetic resonance of $Xe^{129}(^3P_2)$, $Xe^{131}(^3P_2)$ corresponding to F = 5/2, J = 2, I = 1/2 and F - 3/2, J - 2, I = 1/3 respectively, and even $Xe^+(^2P_{3/2})$ as well as the resonance of the state, not yet identified, with rf frequency of 9.2498 MHz

Fig. 5. Magnetic resonance of $Xe^{131}(^3P_2)$ with F = 3/2, J = 2, I = 3/2 with rf frequency of 13.60843 MHz

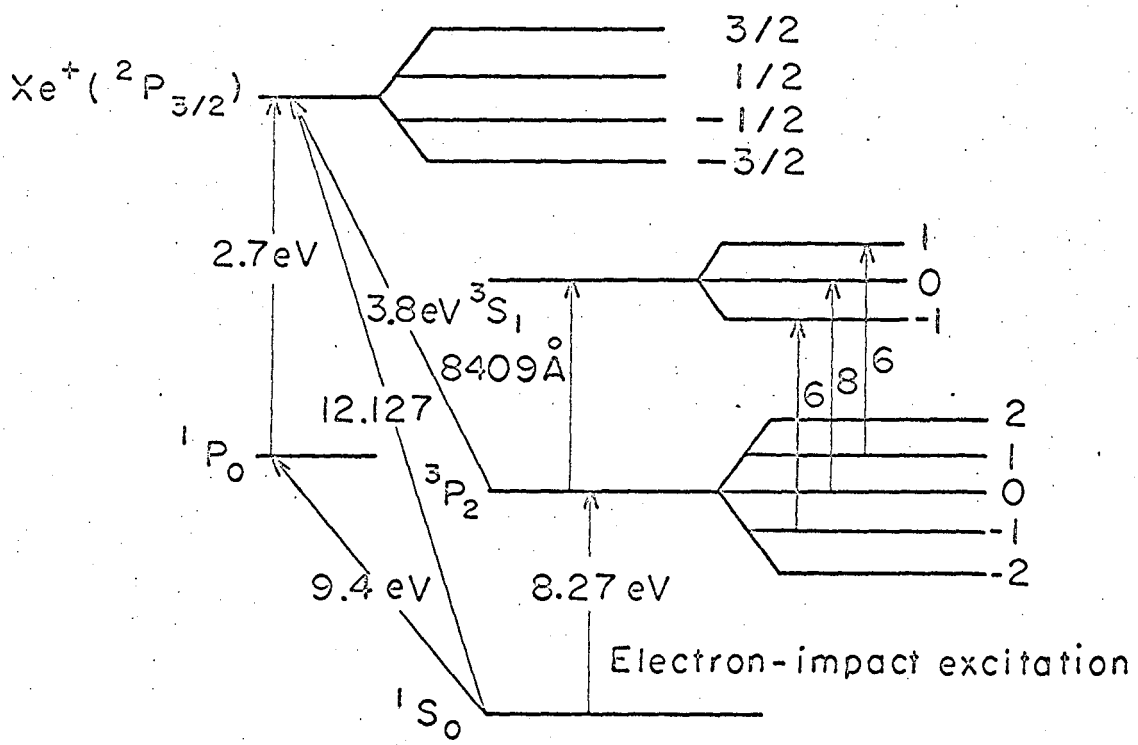

Relevant energy level used in Xe ($^3P_2$) resonance absorption

MUB-14108-A

Fig. 1

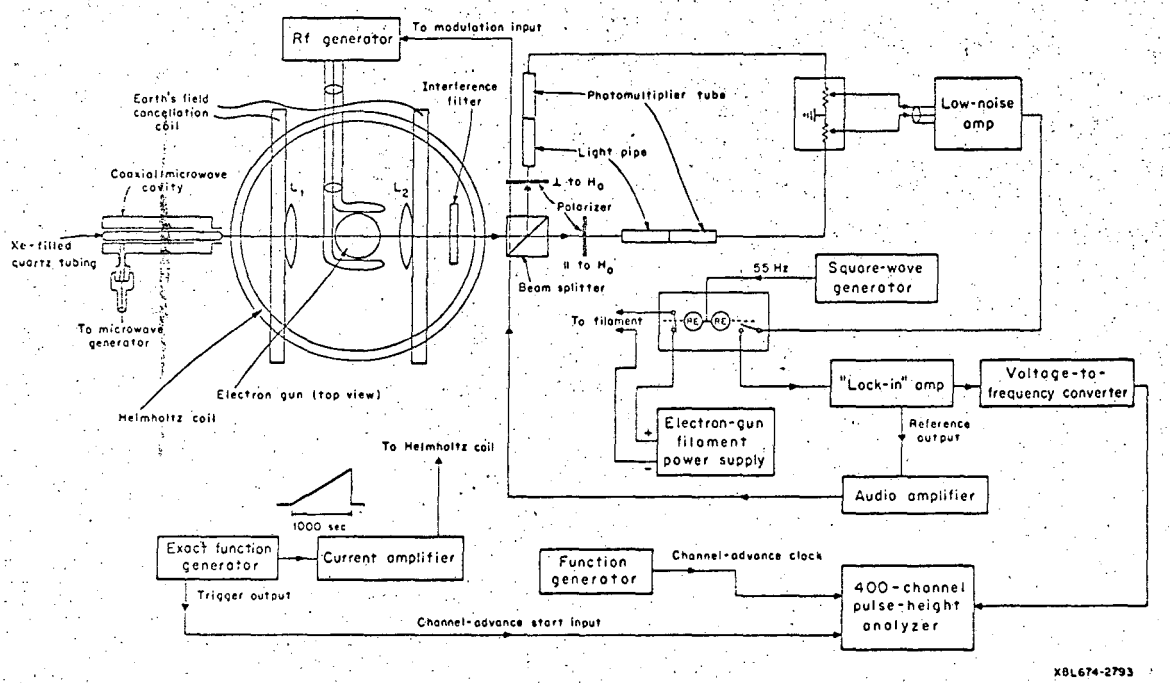
Rf generator
To modulation input
Earth's field cancellation coil
Interference filter
Photomultiplier tube
Low-noise amp
Light pipe
Coaxial microwave cavity
⊥ to H_0
Polarizer
L_1
L_2
Xe-filled quartz tubing
∥ to H_0
Beam splitter
55 Hz
Square-wave generator
To filament
To microwave generator
"Lock-in" amp
Voltage-to-frequency converter
Electron gun (top view)
Helmholtz coil
Electron-gun filament power supply
Reference output
To Helmholtz coil
Audio amplifier
1000 sec
Exact function generator
Current amplifier
Function generator
Channel-advance clock
400-channel pulse-height analyzer
Trigger output
Channel-advance start input
XBL674-2793

Fig. 2

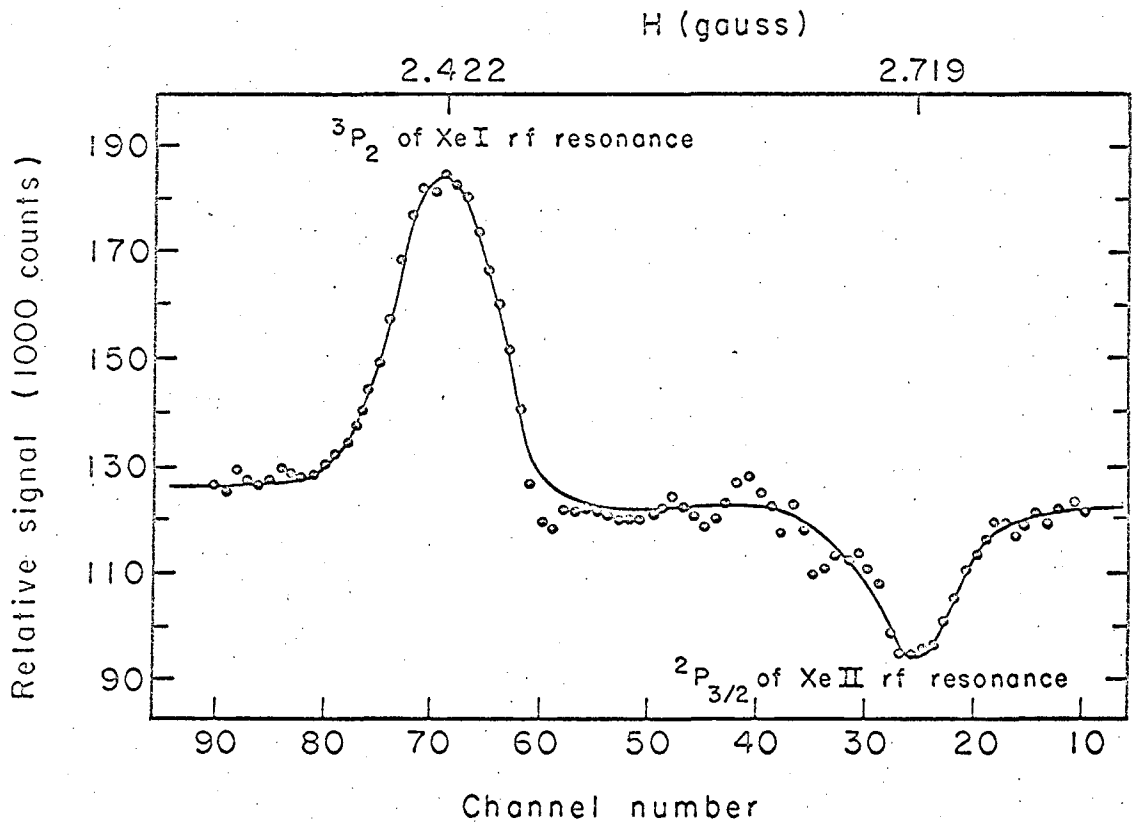

MUB-11917

Fig. 3

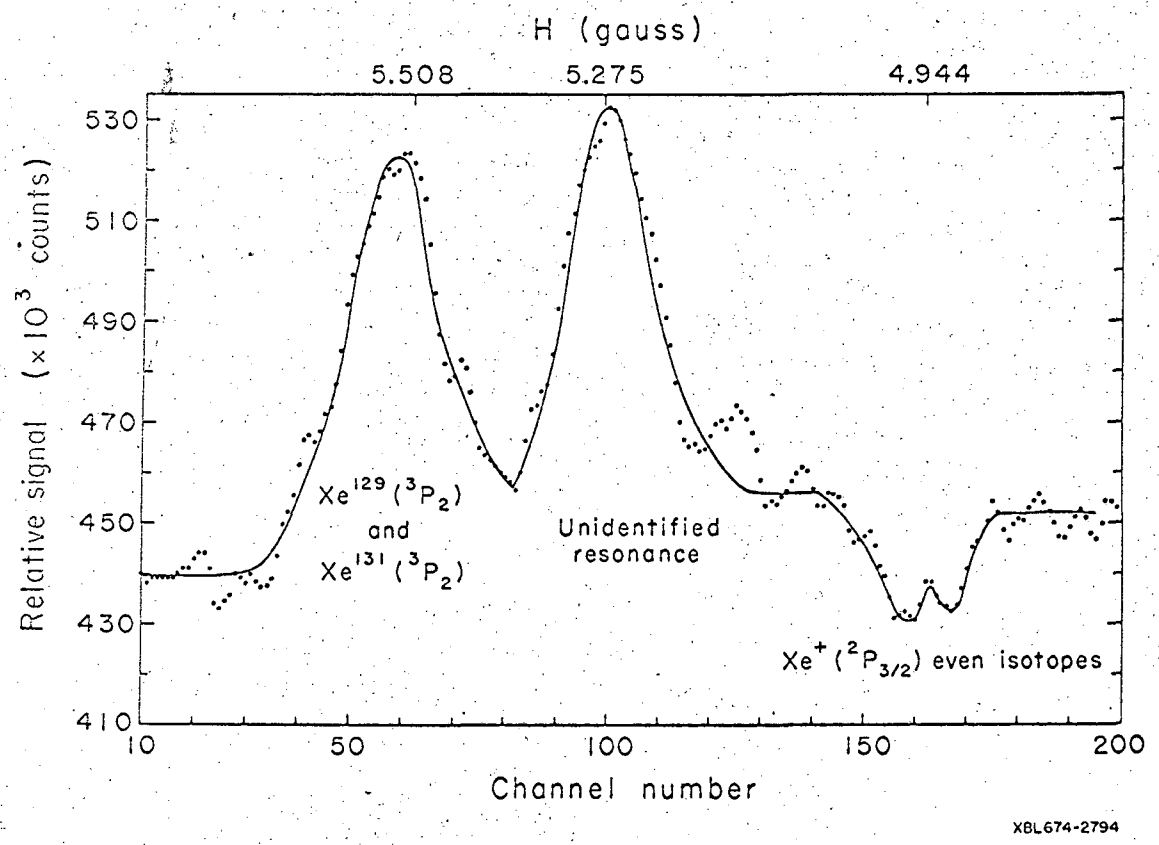
H (gauss)
5.508
5.275
4.944
530
510
490
470
450
430
410
Relative signal (x 10^3 counts)
Xe^129 (^3P_2)
and
Xe^131 (^3P_2)
Unidentified
resonance
Xe^+ (^2P_3/2) even isotopes
10
50
100
150
200
Channel number
XBL674-2794

Fig. 4

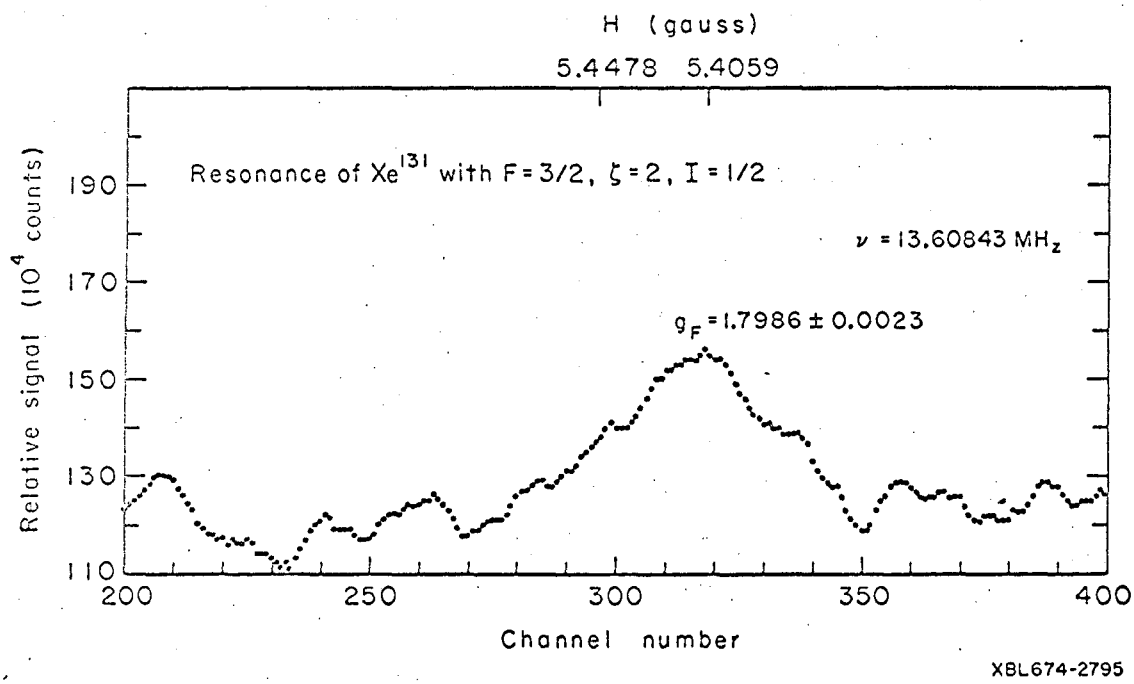
H (gauss)
5.4478 5.4059
Resonance of Xe131 with F=3/2, ζ=2, I=1/2
ν = 13.60843 MHz
gF = 1.7986 ± 0.0023
Relative signal (10^4 counts)
190
170
150
130
110
200
250
300
350
400
Channel number
XBL674-2795

Fig. 5

This report was prepared as an account of Government sponsored work. Neither the United States, nor the Commission, nor any person acting on behalf of the Commission:

A. Makes any warranty or representation, expressed or implied, with respect to the accuracy, completeness, or usefulness of the information contained in this report, or that the use of any information, apparatus, method, or process disclosed in this report may not infringe privately owned rights; or

B. Assumes any liabilities with respect to the use of, or for damages resulting from the use of any information, apparatus, method, or process disclosed in this report.

As used in the above, "person acting on behalf of the Commission" includes any employee or contractor of the Commission, or employee of such contractor, to the extent that such employee or contractor of the Commission, or employee of such contractor prepares, disseminates, or provides access to, any information pursuant to his employment or contract with the Commission, or his employment with such contractor.